between numbers of counts. That is, if a detector records N counts in time t, the counting rate is N/t with an uncertainty of $N^{1/2}/t$. If we wish to subtract B background counts, the uncertainty in the difference $N - B$ is $(N + B)^{1/2}$, following the usual rules for propagation of error.

7.6 ENERGY MEASUREMENTS

A schematic diagram of the equipment that might be used to measure the energy of nuclear radiations is shown in Figure 7.23. The electronic signal from the detector usually goes directly to a *preamplifier* (preamp), which converts the charge pulse from the detector to a voltage pulse (for example, by charging a capacitor) and then drives the pulse to the next element in the circuit. The *amplifier* provides the voltage gain to bring the millivolt preamp pulse to the range of a few volts where it can conveniently be processed. The amplifier must be *linear*, so that the proportionality of radiation energy and pulse height can be preserved. The many pulse heights that may be produced by a complex decay process can conveniently be displayed on a *multichannel analyzer* (MCA) in histogram style, that is, with pulse height on the horizontal scale and number of pulses on the vertical. The input pulses are digitized, and the digital pulse height is stored in a memory location referred to as a *channel*; hence, the horizontal axis is often labeled as *channel number*. The resulting pulse-height *spectrum* can then be used to determine the energies of the radiations emitted by the source (from their locations on the horizontal scale) and their relative intensities (from the areas of the various peaks in the spectrum). This is most frequently done for γ radiation, which is now discussed in more detail.

Figure 7.24 shows some of the processes that can occur when a γ-ray photon enters a solid detector. The photon can Compton scatter several times; after each scattering, the photon loses some energy and a free electron is produced. Gradually the photon suffers either of two fates: it continues the repeated Compton scattering, eventually becoming so low in energy that photoelectric absorption occurs and the photon vanishes, or else it wanders too close to the edge of the crystal and scatters out of the crystal. The energy of the photon is converted into electrons (photoelectrons or Compton-scattered electrons), which have a very short range in the crystal, and which therefore lose energy very rapidly, by creating light photons in a scintillator or electron-hole pairs in a

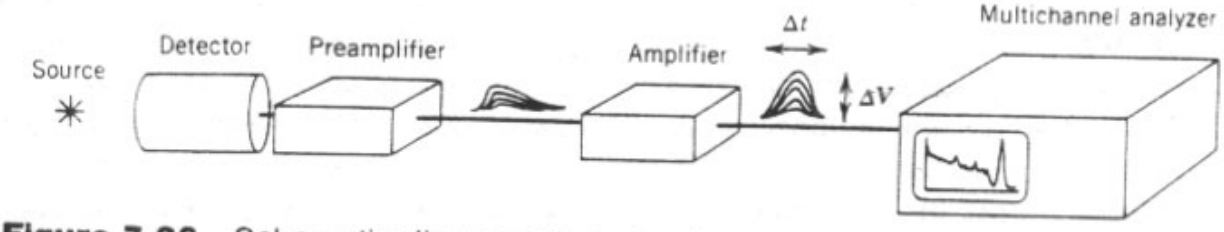

Figure 7.23 Schematic diagram of electronic equipment that might be used in a measurement of the energies of radiations emitted by a source. The pulses between the preamplifier and amplifier generally have a short (ns) rise time and a long (ms) decay time, with an amplitude of millivolts. The amplifier pulses are more symmetric, with a width Δt of μs and a pulse height ΔV of a few volts. The multichannel analyzer display shows ΔV on the horizontal axis.

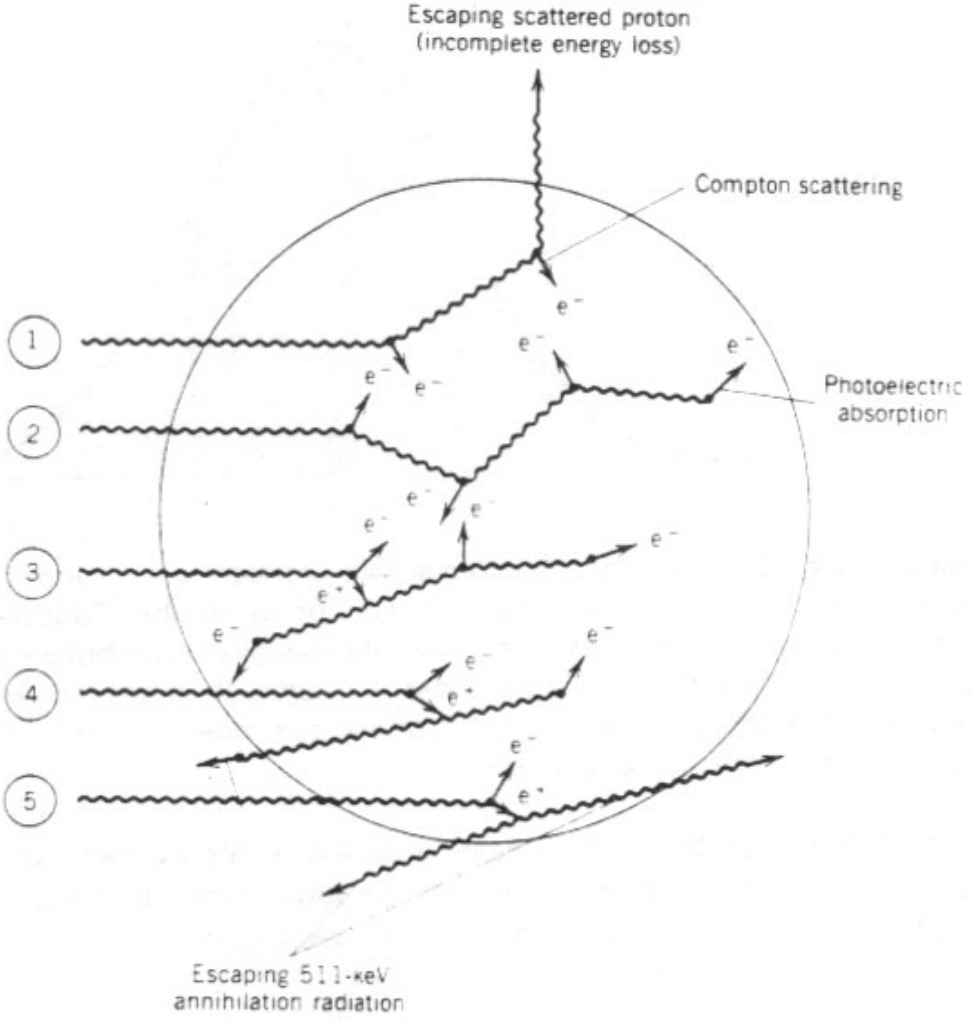

Figure 7.24 Processes occurring in γ-ray detection. (1) The photon Compton scatters a few times and eventually leaves the detector before depositing all its energy. (2) Multiple Compton scattering is followed by photoelectric absorption, and complete energy deposition occurs. (3) Pair production followed by positron annihilation, Compton scattering, and photoelectric absorption; again, complete energy loss occurs. (4) One of the annihilation photons leaves the detector, and the γ ray deposits its full energy less 511 keV. (5) Both annihilation photons leave the detector, resulting in energy deposition of the full energy less 1022 keV. Processes (4) and (5) occur only if the γ-ray energy exceeds 1022 keV.

semiconductor detector. We can assume that all of this energy is absorbed, and we will refer to this quantity as the energy deposited in the detector by the original photon. If the original photon eventually suffers photoelectric absorption, the energy deposited is equal to the original γ-ray energy. If it scatters out of the crystal, the energy deposited is less than the original photon energy.

Let's consider how much energy is given to the scattered electron in a single Compton event. From Equation 7.15, we can find the electron kinetic energy:

$$T_e = E_\gamma - E'_\gamma = \frac{E_\gamma^2(1 - \cos\theta)}{mc^2 + E_\gamma(1 - \cos\theta)} \tag{7.31}$$

Since all scattering angles can occur in the detector, the scattered electron ranges in energy from 0 for $\theta = 0°$ to $2E_\gamma^2/(mc^2 + 2E_\gamma)$ for $\theta = 180°$. These electrons will normally be totally absorbed in the detector, and (if the scattered photons escape) they contribute to the energy response of the detector a continuum called

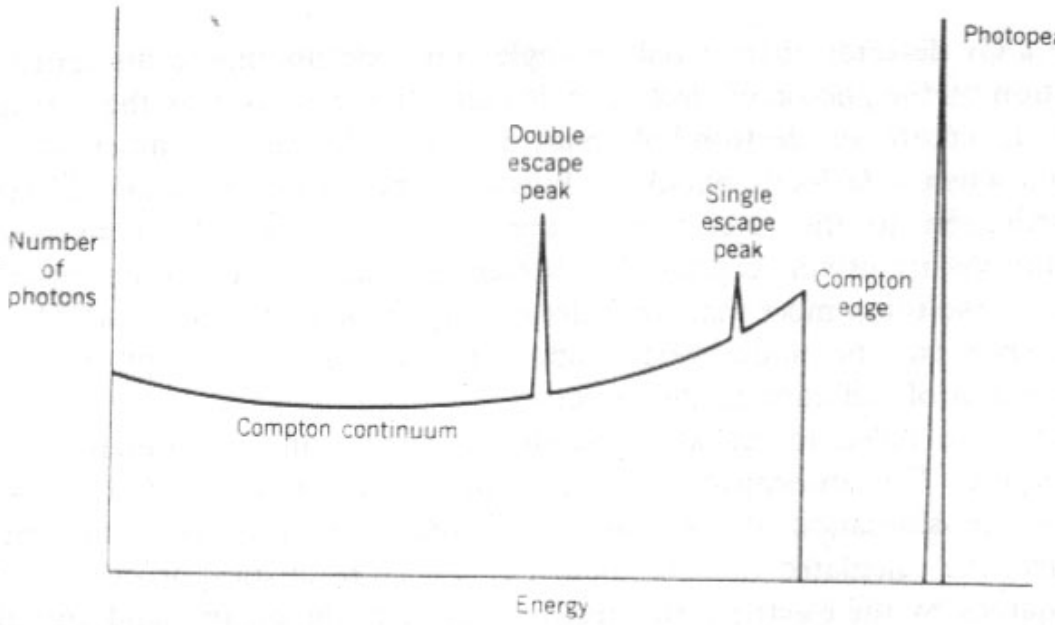

Figure 7.25 A typical response of a detector to monoenergetic γ rays. The photopeak results from the γ ray losing all its energy in the detector, as in events 2 and 3 in Figure 7.24. The Compton continuum consists of many events of type 1, while the single- and double-escape peaks result from processes 4 and 5. The detector energy resolution might tend to broaden all peaks more than they are shown here, and multiple Compton scattering will fill in the gap between the Compton edge and the photopeak. The escape peaks appear only if the γ-ray energy is above 1.022 MeV.

the *Compton continuum*, ranging from zero up to a maximum known as the *Compton edge*. (This continuum is not flat: the Klein-Nishina formula, Equation 7.16, shows how the Compton scattering probability varies with angle.) The peak at $E = E_\gamma$ corresponding to complete photoelectric absorption (called the *full-energy peak* or *photopeak*) and the Compton continuum are shown in Figure 7.25.

We have so far neglected the third process of γ-ray interactions in the detector, that of pair production. The positron and electron are created with a total kinetic energy of $E_\gamma - 2mc^2$, as in Equation 7.18, and loss of that energy in the detector would result in a peak at the full energy. However, once the positron slows down to an energy near that of the atomic electron, *annihilation* takes place, in which the positron and an atomic electron disappear and are replaced by two photons of energy mc^2 or 511 keV. These two photons can travel out of the detector with no interactions, or can be totally or partially absorbed, through Compton scattering processes. We therefore expect to see peaks at $E_\gamma - 2mc^2$ (when both photons escape), $E_\gamma - mc^2$ (when one escapes and the other is totally absorbed), and E_γ (when both are totally absorbed). These single- and double-escape peaks are shown in Figure 7.25.

The relative amplitudes of the photopeak, Compton continuum, and escape peaks depend on the size and shape of the detector. In general, the larger the detector, the smaller is the Compton continuum relative to the photopeak, for there is a smaller chance of a Compton-scattered photon surviving from the center to the surface without interacting again. Similarly, in a large detector, there is a greater chance of capturing one or both of the 511-keV annihilation photons.

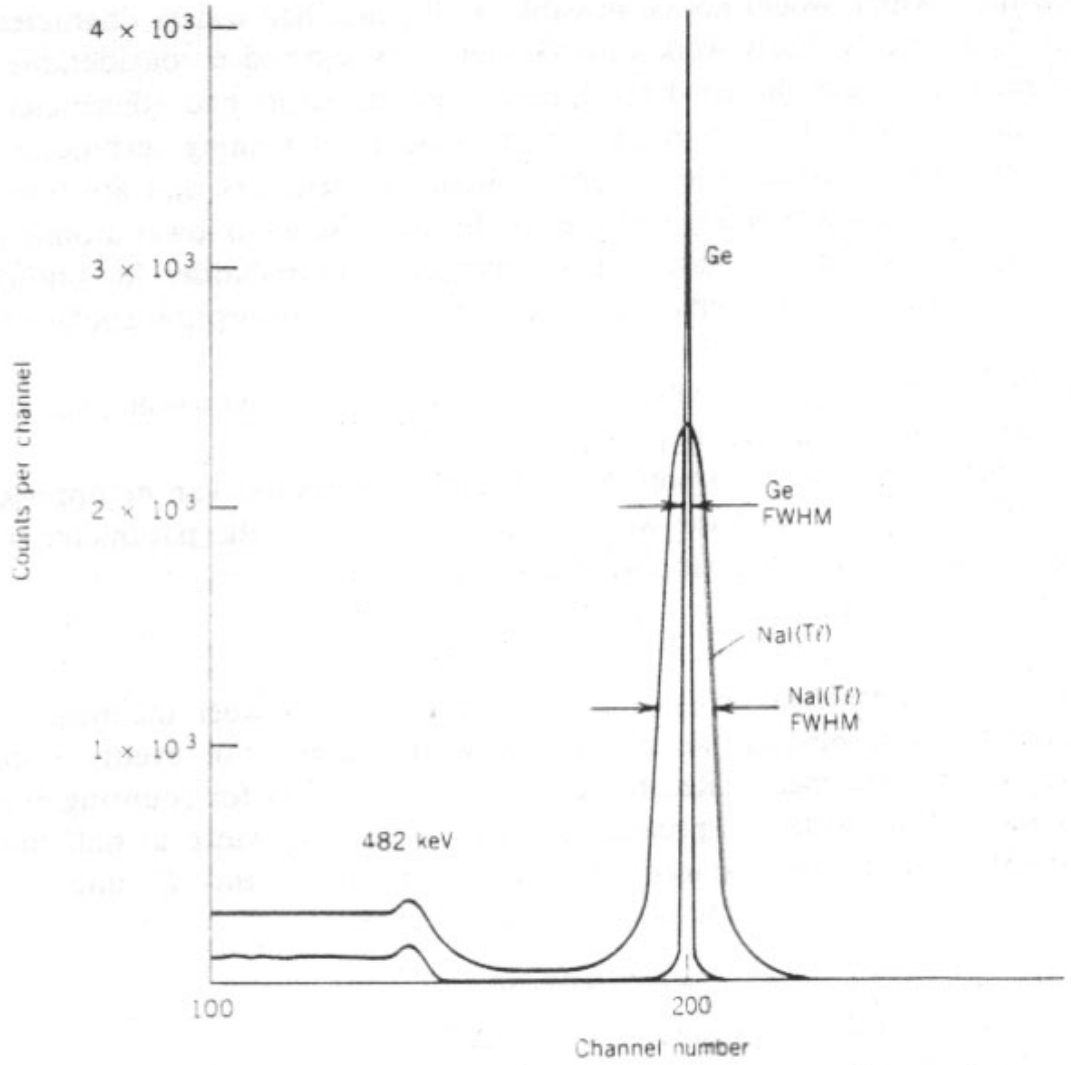

Figure 7.26 Comparison of NaI(Tl) and Ge(Li) spectra of ^{137}Cs. The energy of the photopeak is 662 keV. The resolution (FWHM) of the NaI(Tl) is about 40 keV, while that of the Ge is about 1 keV. The intensity (peak area) of the Ge is about 11% that of NaI(Tl).

Figure 7.26 shows MCA spectra of the decay of ^{137}Cs, such as might be obtained with Ge and NaI(Tl) detectors. Only a single γ ray, of energy 662 keV, is emitted in this decay. The Compton continuum is easily seen, as is the Compton edge. The "valley" between the Compton edge and the photopeak does not go quite to zero and the Compton edge itself is not sharp; in our previous discussion we assumed the Compton continuum to originate from a single-scattering event, and multiple-scattering events will distort the simple picture of Figure 7.25. The Compton edge is expected at $E = 478$ keV, in agreement with the observed spectrum.

What is striking about the two spectra shown are the differences in efficiency (essentially, the area of photopeak) and in resolution (the width of the photopeak) between Ge and NaI(Tl). NaI detectors have higher efficiencies than Ge detectors, and in addition have the advantages of lower cost (1/10 or less of the Ge cost) and simpler operating conditions (no cooling is required for NaI). Because the present demands of nuclear spectroscopy require the study of ever more complex decays, resolution has become of critical importance; to study these decays carefully, one must be able to determine all γ-ray energies and

intensities, which would not be possible if all peaks had widths characteristic of NaI(Tl) detectors. Early work with Ge detectors suffered a considerable loss in efficiency to obtain the good resolution; these detectors had efficiencies only a few percent of NaI(Tl) detectors. Improvements in refining techniques of Ge have enabled the production of large-volume Ge detectors that are now only a factor of 2–3 below NaI(Tl) in efficiency. Because Ge has a lower atomic number than NaI, it will always have smaller interaction probabilities for photons and therefore smaller relative efficiency, the photoelectric absorption coefficient varying roughly as Z^4.

Let's now try to understand the reasons for the observed resolutions based on the statistics of the detection process.

The full-energy peaks of both NaI(Tl) and Ge detectors can be approximated as Gaussian shapes, and the width is characterized by the parameter σ in the general form of the Gaussian distribution

$$f(E) = A\,e^{-(E-\bar{E})^2/2\sigma^2} \tag{7.32}$$

where A is a normalization constant. The relationship between the mean $\bar{E}$ and σ cannot be used because we do not know the number of events $\bar{n}$ that are represented in the mean. (Recall that $\sigma = \sqrt{\bar{n}}$ holds only for counting events.)

Generally the width is specified in terms of the full width at half maximum (FWHM), that is, the distance ΔE between the two points E_1 and E_2 where $f(E_1) = f(E_2) = A/2$. A bit of manipulation gives

$$\Delta E = 2\sigma\sqrt{2\ln 2} \cong 2.35\sigma \tag{7.33}$$

Often the FWHM is expressed as a ratio $\Delta E/\bar{E}$.

To estimate σ, we must estimate $\bar{n}$, the number of statistical events associated with the production of the detector signal. The incident γ-ray energy is 662 keV. In NaI(Tl) the scintillation efficiency (the fraction of the incident radiation converted into light) is about 13%; thus 86 keV of photons appear. The energy per photon in NaI is about 4 eV, and the number of light photons is thus (on the average) about 21,000. The contribution to the resolution from this is about $2.35\sqrt{21{,}000}/21{,}000$ or about 1.6%. At the photocathode, the number is reduced even further. The transmission of the light through the glass end of the photomultiplier tube is typically about 85%, and the *quantum efficiency* of a typical photocathode (that is, the number of photoelectrons emitted per incident photon) is typically 23%. Thus the number of photoelectrons is only about 20% of the number of incident photons, or about 4200, and the contribution to the resolution is about $2.35\sqrt{4200}/4200$, or 3.6%. The electron multiplication process in the photomultiplier will increase the number of events and give a smaller contribution to the FWHM. *In the entire NaI(Tl) detection process, the smallest number of events corresponds to the production of electrons at the photocathode, and this is therefore the most substantial contributor to the energy resolution.*

This simple calculation has ignored a number of effects in the crystal, photomultiplier, and amplifier, all of which can make nonstatistical contributions to the resolution. A figure of 6% (40 keV) might be more typical at 662 keV. The absolute FWHM (the width of the energy peak) increases with energy, roughly as $E^{1/2}$, but the ratio $\Delta E/E$ decreases like $E^{-1/2}$; thus at 1 MeV, the resolution should be about 5% (50 keV).

In a Ge detector, there is only a single event contributing to the statistics—the creation by the photon of electron-hole pairs. In Ge, it takes on the average about 3 eV to create an electron-hole pair, and thus the mean number of statistical events when a 662-keV photon is fully absorbed would be about 220,000. The contribution to the resolution is then about 3.3 keV (by convention, NaI resolutions are usually expressed as percentages, and Ge resolutions in keV). This gives a resolution more than an order of magnitude better than NaI(Tl), and this difference can be understood simply on the basis of the properties of the absorption of radiation in the detectors.

We have failed to include a number of factors in our estimate for the Ge resolution. The absorption is in fact not well described by Poisson statistics; proper consideration of the statistical nature of the process (done empirically) reduces the calculated value to about 1.0 keV. Nonstatistical processes (collection of charges by the electric field, electronic noise in the preamp and amplifier) will tend to increase the value somewhat. A typical value for a good detector today is 1.7 keV at 1332 keV (the energy of a ^{60}Co γ-ray, taken as the standard for resolution measurement), which would correspond to about 1.2 keV at 662 keV, if the $E^{1/2}$ dependence is valid.

In γ-ray (or other radiation) spectroscopy measurements, the goal is usually to determine the energy and the intensity of the radiation. To find the energy, the centroid of a peak must be determined. For isolated, well-resolved peaks, the centroid can be determined by a simple numerical procedure. First it is necessary to subtract the background. (The peak may be on the Compton continuum of other peaks higher in energy.) This is usually done by drawing a straight line between groups of background channels above and below the peak (Figure 7.27). In this case a linear background is assumed, and the background counts can be

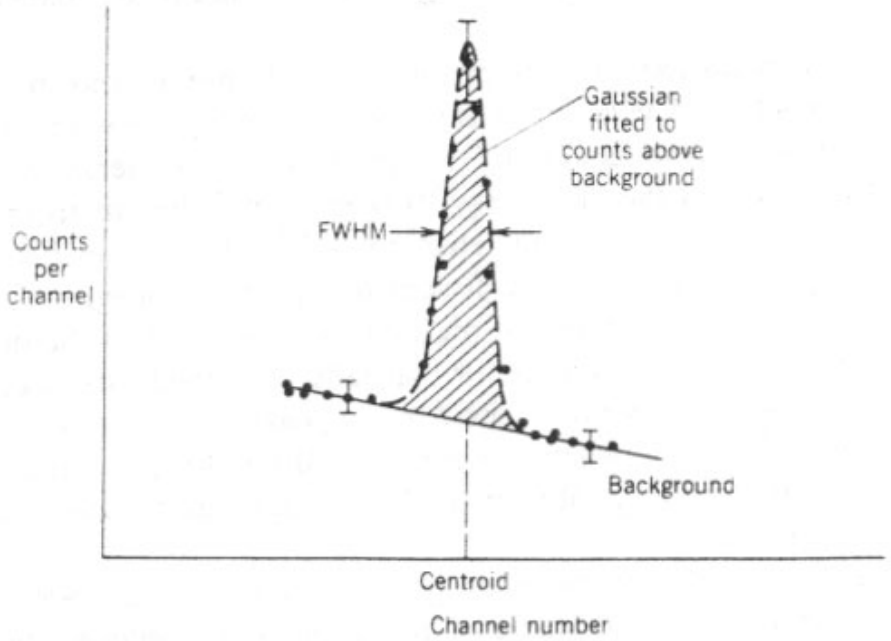

Figure 7.27 The area of a well-resolved peak can be found by subtracting a linear background and then either adding the counts above background or fitting a Gaussian function to the counts above background. Because the number of counts in each channel results from a simple counting process, its uncertainty is just the square root of the number; this applies only to the total number in each channel and *not* to the number above background.

subtracted directly. The centroid and area can then be determined by

$$\text{area} = \sum y_i \tag{7.34}$$

$$\text{centroid} = \frac{\sum x_i y_i}{\sum y_i} \tag{7.35}$$

where y_i represents the net number of counts above background in channel i. A slightly more sophisticated method is to fit a Gaussian function to the peak. This can be done most easily by assuming the functional dependence of the form of Equation 7.32 and taking the logarithm:

$$\ln y_i = \ln A - \frac{(x_i - \bar{x})^2}{2\sigma^2} \tag{7.36}$$

A least-squares fit to this form gives the parameters $\bar{x}$, σ, and A. Integrating the Gaussian form gives

$$\text{area} = \sigma A \sqrt{2\pi} \tag{7.37}$$

In the case of complicated spectra, this simple procedure will not work. Often backgrounds are not at all well represented by the linear approximation. Close-lying peaks that may overlap cannot be fitted in this way. Even the assumption of a Gaussian shape is not always valid, as there may be exponential "tails" on the high-energy or low-energy sides of the Gaussian. In this case, there are sophisticated fitting programs that can handle many parameters, including centroids and areas of many peaks and backgrounds of nonlinear shape.

Once we have values for the centroid and area of a peak, we would like to use those values to obtain the energy and counting rate for the radiation. To find the energy, it is necessary to calibrate the MCA so that channel number can be converted to energy. This is usually done with two or more radiations of known energy E_1 and E_2, which would be found to have centroids $\bar{x}_1$ and $\bar{x}_2$. It is then

Table 7.2 Commonly Used Energy Calibration Standards

Nuclide	$t_{1/2}$	Radiation	Energy (keV)
^{109}Cd	453 d	γ	88.037 ± 0.005
^{57}Co	271 d	γ	122.06135 ± 0.00013
			136.47434 ± 0.00030
^{198}Au	2.696 d	γ	411.80441 ± 0.00015
^{137}Cs	30.17 y	γ	661.661 ± 0.003
^{60}Co	5.271 y	γ	1173.238 ± 0.015
			1332.513 ± 0.018
^{207}Bi	38 y	e^-	481.65 ± 0.01
			975.63 ± 0.01
^{241}Am	433 y	α	5485.74 ± 0.12
^{226}Ra	1600 y	α	4784.50 ± 0.25
			5489.66 ± 0.30
			6002.55 ± 0.09
			7687.09 ± 0.06

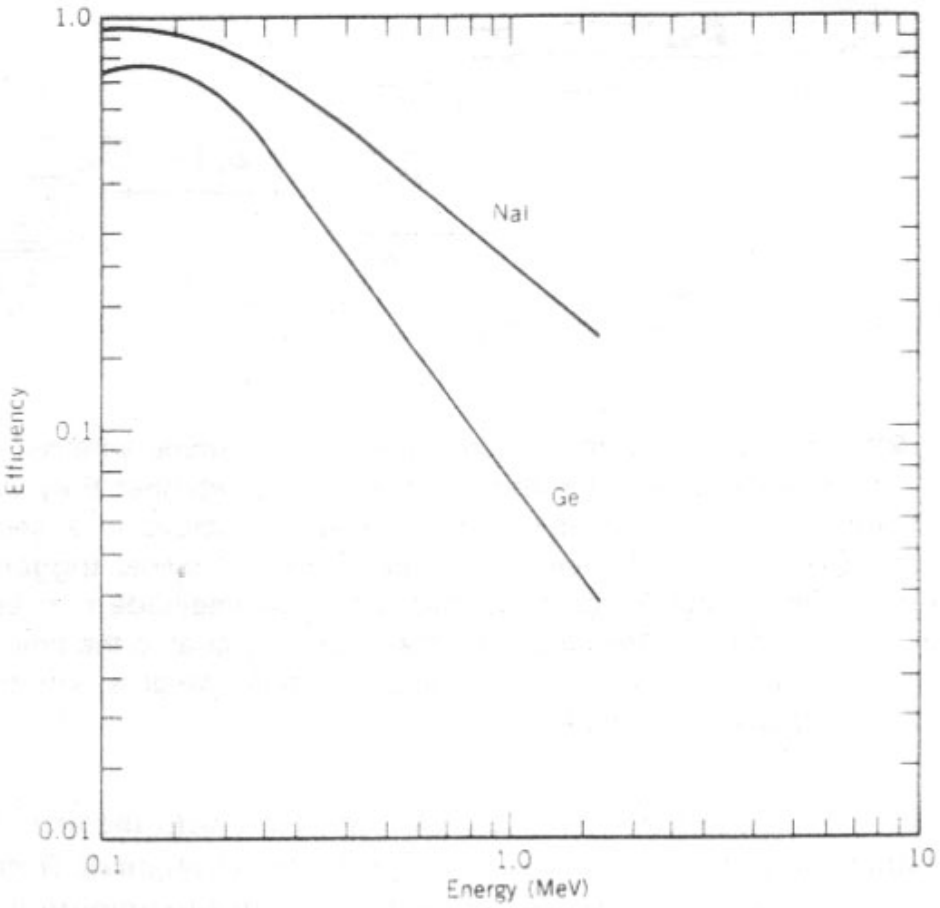

Figure 7.28 Relative efficiencies of NaI and Ge detectors. Here "efficiency" means the probability that a photon *striking the detector* will appear in the photopeak; it does not take into account the differing sizes of the detectors. The curves are drawn for a 3-in.- diameter by 3-in.-long NaI(Tl) and a 4.2-cm-diameter by 4.2-cm long Ge, with the source at 10 cm from the detector. In the terms that are usually used to specify relative efficiencies, the relative probability for a 1.332-MeV photon (emitted by ^{60}Co) to appear in the Ge photopeak is 8% that of the NaI(Tl) photopeak, including the solid angle factor.

easy to find a linear relationship between $\bar{x}$ and E. Because MCAs (and other parts of the system, including the detector and amplifier) may be slightly nonlinear, it is advisable to choose calibration energies E_1 and E_2 as close as possible to the unknown energy E. It is necessary to use two radiations for calibration because channel zero of the MCA will not necessarily correspond to a pulse height of zero. Table 7.2 shows some commonly used calibration standards.

To convert the peak area to an absolute counting rate, we must know something about the efficiency of the detector—how large a solid angle does it subtend at the source of the radiation and what is the probability that an incident radiation will be absorbed into the photopeak? The detector efficiency depends on the energy rather dramatically for γ rays; Figure 7.28 shows the absolute efficiency of NaI(Tl) and Ge detectors as a function of the γ-ray energy.

7.7 COINCIDENCE MEASUREMENTS AND TIME RESOLUTION

When we wish to study radiations that follow one another in cascade—for example, γ rays that follow a particular β decay—equipment of the type shown in Figure 7.29 is often used. One primary object of this equipment is to determine